Eur. Radiol. 10, 832–840 (2000)

European
Radiology

Pictorial review

Osteochondroma: MR imaging of tumor-related complications

K. Woertler[1], **N. Lindner**[2], **G. Gosheger**[2], **C. Brinkschmidt**[3], **W. Heindel**[1]

[1] Department of Clinical Radiology, Westfalian Wilhelms University of Muenster, Albert Schweitzer Strasse 33, D-48129 Muenster, Germany
[2] Department of General Orthopedics, Westfalian Wilhelms University of Muenster, Albert Schweitzer Strasse 33, D-48129 Muenster, Germany
[3] Gerhard Domagk Institute of Pathology, Westfalian Wilhelms University of Muenster, Albert Schweitzer Strasse 33, D-48129 Muenster, Germany

Received: 16 July 1999; Revised: 27 September 1999; Accepted: 29 September 1999

Abstract. Osteochondromas can be complicated by mechanical irritation, compression or injury of adjacent structures, fracture, malignant transformation, and postoperative recurrence. Magnetic resonance imaging represents the most valuable imaging modality in symptomatic cases, because it can demonstrate typical features of associated soft tissue pathology, which can be differentiated from malignant transformation. Reactive bursae formation presents as an overlying fluid collection with peripheral contrast enhancement. Dislocation, deformation, and signal alterations of adjacent soft tissue structures can be observed in different impingement syndromes caused by osteochondromas. Magnetic resonance imaging provides excellent demonstration of arterial and venous compromise and represents the method of choice in cases with compression of spinal cord, nerve roots, or peripheral nerves, depicting changes in size, position, and signal intensity of the affected neural structures. Malignant transformation as the most worrisome complication occurs in approximately 1 % of solitary and 5–25 % of multiple osteochondromas. Magnetic resonance imaging is the most accurate method in measuring cartilage cap thickness, which represents an important criterion for differentiation of osteochondromas and exostotic (low-grade) chondrosarcomas. Cartilage cap thickness exceeding 2 cm in adults and 3 cm in children should raise the suspicion for malignant transformation. Finally, MR imaging can detect postoperative recurrence by depiction of a recurrent mass presenting typical morphological features of a cartilage-forming lesion.

Key words: Osteochondroma – Complications – Chondrosarcoma – Bone tumors – MRI

Correspondence to: K. Woertler

Introduction

Osteochondromas, also termed osteocartilaginous exostoses, are benign cartilage-forming lesions which account for 10–15 % of all bone tumors and apparently occur in 3 % of the population overall [1, 2, 3, 4]. They represent pedunculated or sessile osseous excrescenses in continuity with the marrow and cortex of their host bone, covered by a cartilage cap which usually ossifies with skeletal maturity [1, 2, 3, 4]. On occasion, remnants of a quiescent cartilage cap may persist far into adult life [5]. The pathogenesis of this entity remains speculative. Some investigators consider osteochondromas to be true neoplasms; others believe them to represent growth defects in the perichondrium, covering the epiphyseal plate [2, 3]. Occasionally, an osteochondroma can arise at a site of prior radiation therapy [3]. Solitary osteochondromas show a predilection for the metaphyses of the long tubular bones, especially the femur, humerus, and tibia, but have been described in virtually every part of the skeleton [2, 4]. Multiple osteochondromas occur as part of a rare familial syndrome with autosomal dominant inheritance, termed hereditary multiple exostoses [2, 3].

Most solitary and multiple osteochondromas are discovered during childhood and are usually asymptomatic. However, several potential tumor-related complications can occur especially in lesions with marked extent or location in critical anatomic sites. Clinical symptoms can result from mechanical irritation or compression of adjacent structures (soft tissues, bone, internal organs, peripheral nerves, spinal cord, blood vessels), fracture, and malignant transformation [2, 6].

In this review we present the MR imaging appearance of symptomatic osteochondromas on the basis of pathologically confirmed cases from the files of our bone tumor registrar, which currently contains approximately 2600 cases of cartilage-forming bone tumors, among these 1090 osteochondromas and 380 chondrosarcomas.

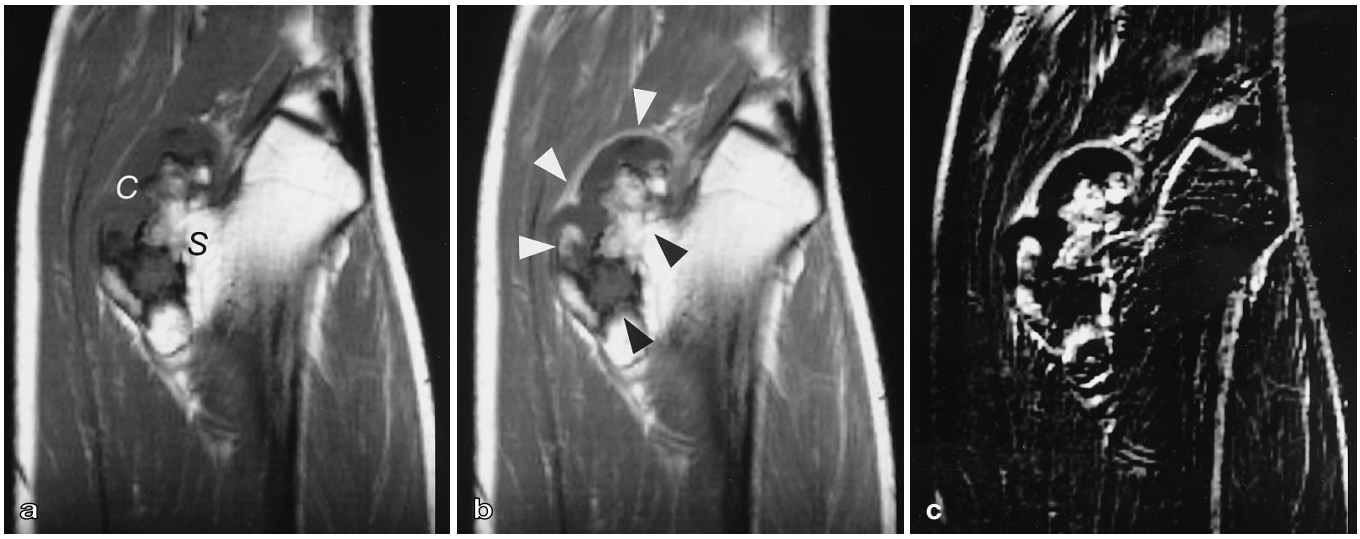

Fig. 1 a–c. Osteochondroma of the fibula in a 23-year-old patient. **a** Paracoronal T1-weighted spin-echo (SE) image shows the osseous stalk *(S)* of the osteochondroma in continuity with bone marrow and cortex of the fibula, covered by the cartilage cap *(C)*. On **b** corresponding contrast-enhanced T1-weighted image and especially **c** subtraction image peripheral "ring-and-arc" as well as "nodular" enhancement are observed *(arrows)*. Histopathology showed typical features of an osteochondroma without evidence of malignant transformation

Fig. 2 a–c. A 28-year-old female patient with enlarging mass in the right axilla. Sagittal oblique **a** T1-weighted, **b** contrast-enhanced T1-weighted, and **c** axial T2-weighted SE images show an osteochondroma originating from the inferior angle of the scapula *(arrow)* as well as an encapsulated fluid collection *(arrowheads)* with marked peripheral contrast enhancement. Surgery confirmed an inflamed bursa overlying the osteochondroma with no evidence of chondrometaplastic change. Note hyperintense signal of fluid on T1-weighted MR images due to high protein content as well as irregular bursal sac thickening caused by hyperplastic pseudosynovium

General features

The overall morphology of osteochondromas can clearly be demonstrated by MR imaging. MR shows continuity of the exostotic bone marrow and cortex with that of the underlying bone (Fig. 1), allowing differentiation against other juxtacortical lesions [3, 5]. The covering cap can be identified with typical signal characteristics of hyaline cartilage: low to intermediate signal intensity on T1- and high signal intensity on T2/T2*-weighted and short tau inversion recovery (STIR) images, and frequently it is lined by a superficial zone of low signal intensity, which most likely represents an intact perichondrium [5]. The high signal intensity of the cartilage covering, observed on T2-weighted images, is presumed to be related to the high water content of hyaline cartilage in relation to its mucopolysaccharide component [7]. Gadolinium-enhanced T1-weighted images can show delicate, predominantly peripheral enhancement, corresponding with fibrovascular tissue covering the

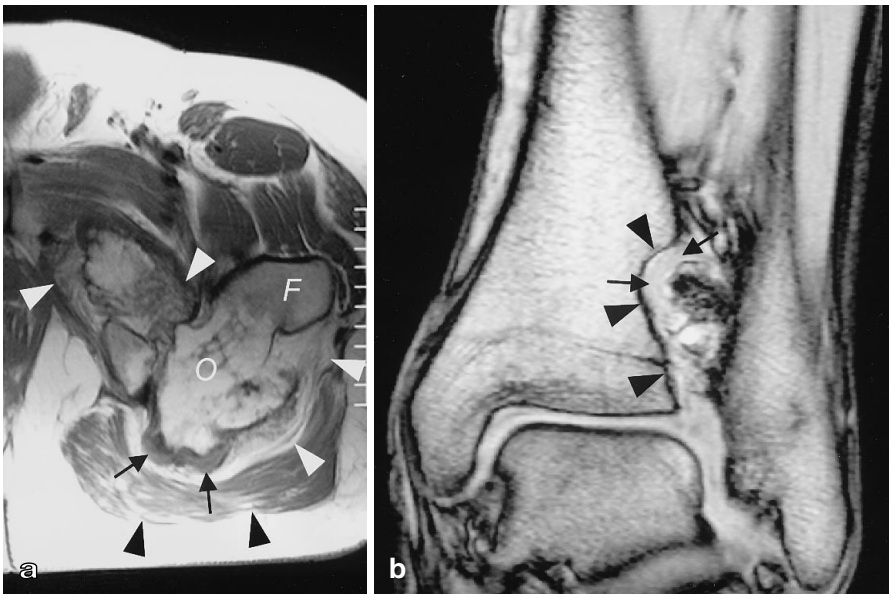

Fig. 3 a, b. Musculoskeletal sequelae. **a** Fatty atrophy of adjacent muscles *(arrowheads)* in a patient with large osteochondroma *(O)* of the femur *(F)*, covered by a thin cartilage cap (*arrows*; axial T1-weighted SE image). **b** Pressure erosion of the distal tibia *(arrowheads)* caused by an osteochondroma of the fibula. Note hyperintense signal of cartilage cap *(arrows)* on coronal T2*-weighted gradient-echo image

non-enhancing hyaline cartilage [8]. Calcifications of the cartilaginous matrix normally present as regions of signal loss on images of all pulse sequences. After complete ossification with cortical and medullary bone formation the former cap often remains distinguishable from the pedicle by a hypointense line, resembling a fused growth plate.

In our current MR imaging protocol for bone tumors we routinely perform pre- and post-contrast T1-weighted spin-echo (SE) sequences in the coronal or sagittal plane as well as axially oriented proton-density/T2-weighted SE and post-contrast fat-suppressed T1-weighted SE sequences. In cases of osteochondromas the imaging plane along the long axis of bone usually has to be modified depending on the orientation of the osteochondroma (paracoronal/parasagittal) in order to depict the full extent of the lesion. Long axis images after contrast administration are obtained without fat suppression, because in our experience subtle enhancement occurring in well-differentiated cartilage-forming lesions is often more easily identified on non-fat-suppressed or subtraction images (Fig. 1), probably due to the increased signal intensity of hyaline cartilage with fat suppression. The reason for using conventional SE rather than fat-suppressed fast-spin-echo (FSE) sequences for T2-weighted images is much more of a "philosophic" than a rational one, because both imaging techniques can successfully be performed on solitary bone lesions. However, we believe that T2-weighted conventional SE images still allow a better differentiation of signal intensities within different "bright" structures such as hyaline cartilage and fluid.

Fig. 4 a–c. A 14-year-old male patient with acute pain in the distal thigh after local trauma. **a** Coronal T1-weighted and **b,c** axial T2-weighted SE images demonstrate a pedunculated osteochondroma of the distal femur with a large reactive bursa *(arrowheads)*. Especially on T2-weighted image **(b)** the cartilage cap can be differentiated from overlying bursa fluid. Note bone marrow edema and discontinuity of the stalk *(arrow)* as well as soft tissue edema due to fracture

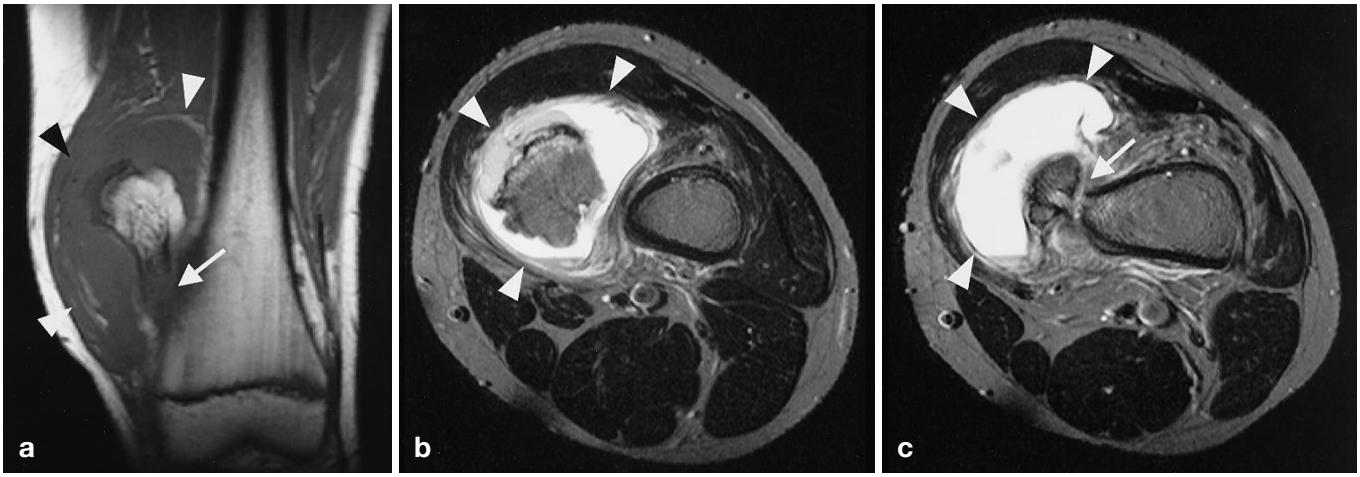

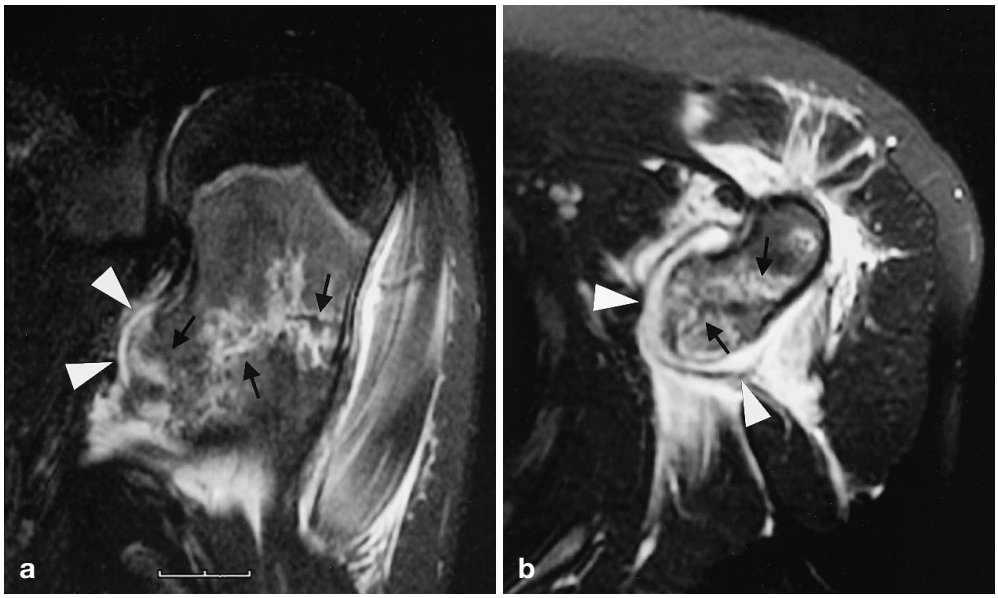

Fig. 5 a, b. A 14-year-old male patient with transverse fracture of the proximal humerus after adequate trauma. **a** Coronal and **b** axial fat-suppressed T2-weighted FSE images show a sessile osteochondroma at the medial aspect of the humeral metaphysis. The hyperintense cartilage cap *(arrowheads)* typically demonstrates a superficial zone of low signal intensity. Fracture lines *(arrows)* extend into the osseous part of the osteochondroma. Note posttraumatic bone marrow edema and extensive edema of surrounding soft tissues. On follow-up the fracture healed under conservative treatment

Musculoskeletal complications

Musculoskeletal complications in patients with osteochondromas can become evident due to chronic mechanical irritation as well as acute trauma. Reactive bursa formation is a well-known sequel, which most often occurs within the shoulder region and which can be complicated by inflammation, infection, hemorrhage, and chondrometaplastic change with loose body formation [4, 6]. The clinical presentation of an enlarging, painful mass can be mistaken for malignant transformation [6]. On MR images a bursa presents as a localized fluid collection overlying the osteochondroma (Figs. 2, 4) [4]. Marked synovial enhancement within the bursa, bursal sac thickening, as well as edema of surrounding soft tissues is observed in cases of inflammation, infection, and hemorrhage [6]. Due to the presence of fibrinous deposits or methemoglobin, the T1 relaxation time of bursa fluid can be shortened, leading to a high signal intensity of fluid content on T1-weighted images (Fig. 2).

Tenosynovitis, tendon snapping, recurrent tendon dislocation, locking or restricted motion of joints, impingement syndromes, muscle injury, and muscular atrophy are further soft tissue effects, which vary depending on the location of the osteochondroma [6, 9]. Due to its multiplanar imaging capabilities and superior soft tissue contrast, MR imaging can be used to determine exactly the relationship of symptomatic osteochondromas to adjacent musculoskeletal structures [9]. Increased T2-weighted signal intensity of overlying muscles, thought to represent edema, has been reported in patients with impingement symptoms caused by osteocartilaginous exostoses of the femur [9]. Furthermore, the presence and extent of muscular atrophy with consecutive lipomatosis can reliably be assessed by MR imaging (Fig. 3 a).

Bone deformity due to growth disturbances and failure of normal tubulation are typical symptoms in patients with hereditary multiple exostoses [3, 6]. However, pressure erosion (Fig. 3 b) and deformity of an adjacent bone can also be observed in patients with solitary osteochondromas [3]. The affection of normal growth plate function can lead to growth retardation, deformity and restricted motion of joints, and premature osteoarthritis [6]. Fracture through the stalk of an osteochondroma is an uncommon complication that usually occurs after local trauma (Fig. 4). Although fibrous nonunion with persistent pain has been described, the majority of these fractures heal without sequelae [10]. On occasion non-pathologic fractures can incidentally involve an osteochondroma which has not been detected previously (Fig. 5) Usually, bone and joint complications in patients with osteochondromas can sufficiently be depicted by means of plain radiography. Magnetic resonance imaging can obtain additional information by demonstrating signs of early osteoarthritis and/or ruling out associated soft tissue pathology or malignant transformation. Extensive soft tissue edema after fracture should not be misinterpreted as a sign of malignancy (Figs. 4, 5).

Thoracic and abdominal complications

Injury to internal organs caused by osteochondromas is extremely rare [6, 11]. Exostoses of the ribs and sternum can cause pleuritic or flank pain due to chronic irritation of the pleura or abrasion of the diaphragm (Fig. 6). Pneumothorax, hematothorax, rupture of pericardium, thoracic outlet syndrome, and dysphagia have been described as rare tumor-related complications [6, 11, 12, 13]. In patients with osteochondromas of the pubic bone the mechanical effect on the bladder may lead to cystitis or hematuria (Fig. 7) [6]. Especially in sites of complex skeletal anatomy MR imaging in addition to radiography can help to establish the diagnosis of a benign osteocarti-

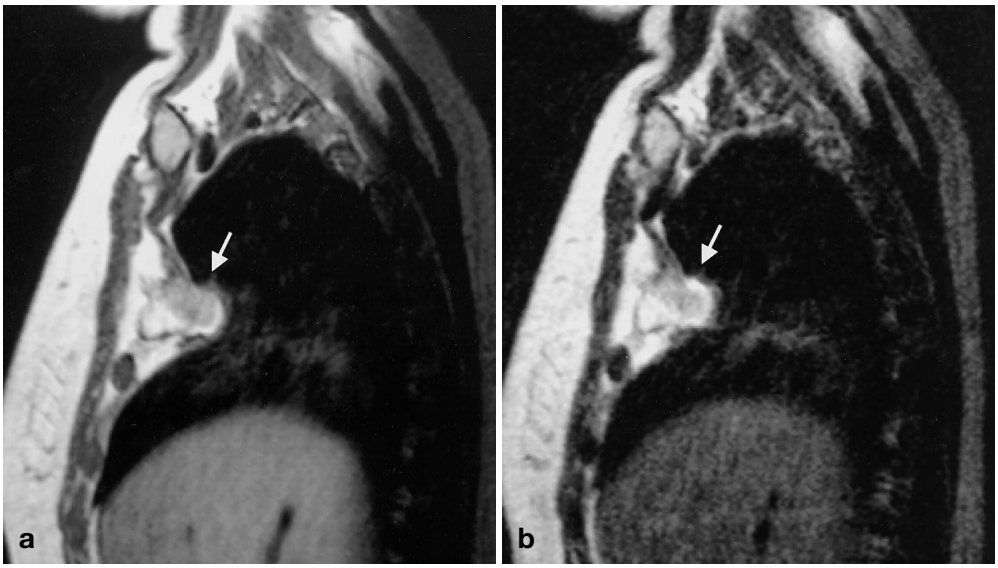

Fig. 6 a, b. A 28-year-old female patient with pleuritic pain caused by a large rib osteochondroma *(arrow)* protruding into the thorax. Sagittal **a** T1-weighted and **b** T2-weighted SE images

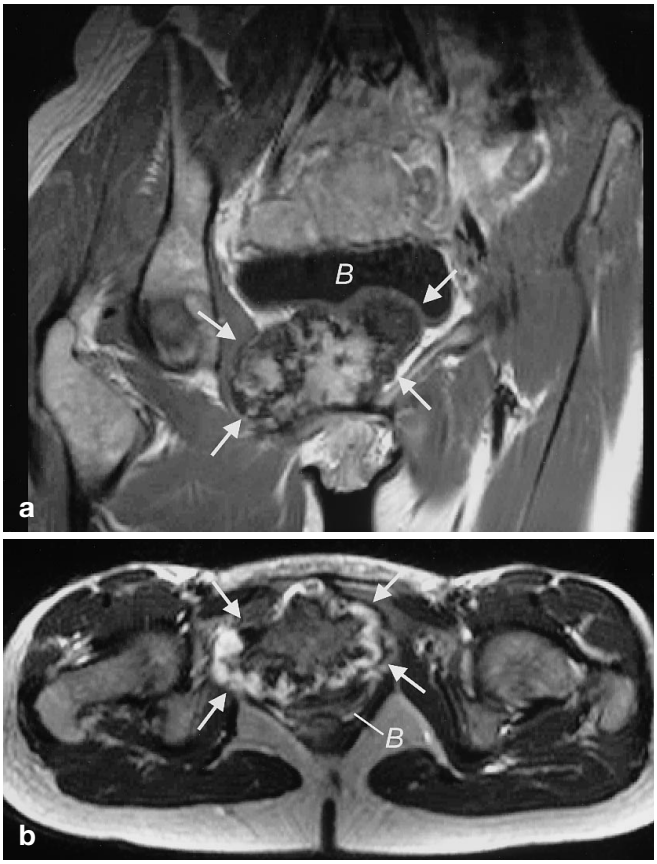

Fig. 7 a, b. A 35-year-old female patient with symptoms of chronic cystitis. **a** Coronal T1-weighted and **b** axial T2-weighted SE images show a large osteochondroma of the pubic bone *(arrows)* compressing the urinary bladder *(B)*

laginous tumor as the cause of the patients' symptoms. Due to its multiplanar capabilities, MR appears to be the best suited imaging modality for demonstrating the relationship of the exostosis to thoracic and abdominal organs (Figs. 6, 7).

Vascular complications

Osteochondromas located close to large vessels can lead to several acute and chronic vascular complications. Arterial injury most commonly involves the popliteal and distal femoral region, where the arteries are relatively fixed in position. Furthermore, the distal femur and proximal tibia and fibula represent common locations for large osteochondromas to occur [14, 15, 16]. Pseudoaneurysm (Fig. 8), arterial thrombosis, thromboembolism, arterial compression with claudication, and transsection have been reported [6, 14, 15, 16]. Venous complications are less frequent sequelae, which include chronic venous compression and thrombosis [14]. Most vascular complications occur at skeletal maturity, as ossification of the cartilaginous cap increases the risk of injury to adjacent vessels [15]. Angiography or Doppler ultrasound are usually required to demonstrate arterial and/or venous complications [14, 17]. On contrast-enhanced CT the thrombosed lumen of a popliteal artery pseudoaneurysm can be misdiagnosed as malignant transformation of the osteochondroma [18]. Magnetic resonance imaging has been shown to provide excellent demonstration of both, arterial and venous compromise. Due to their angiographic effect, gradient-echo sequences proved to be useful in depiction of the anatomic relation between the osteochondroma and compressed vessels [14]. Arterial pseudoaneurysms usually demonstrate inhomogeneous signal intensity caused by blood-breakdown products of different age within thrombosed material and turbulent flow [6], typically resulting in an onion-skin-like, laminated appearance (Fig. 8c) [19, 20].

Neurologic complications

Osteochondromas of the peripheral skeleton can cause nerve compression with consecutive entrapment neuropathies or nerve palsies. The peroneal nerve represents

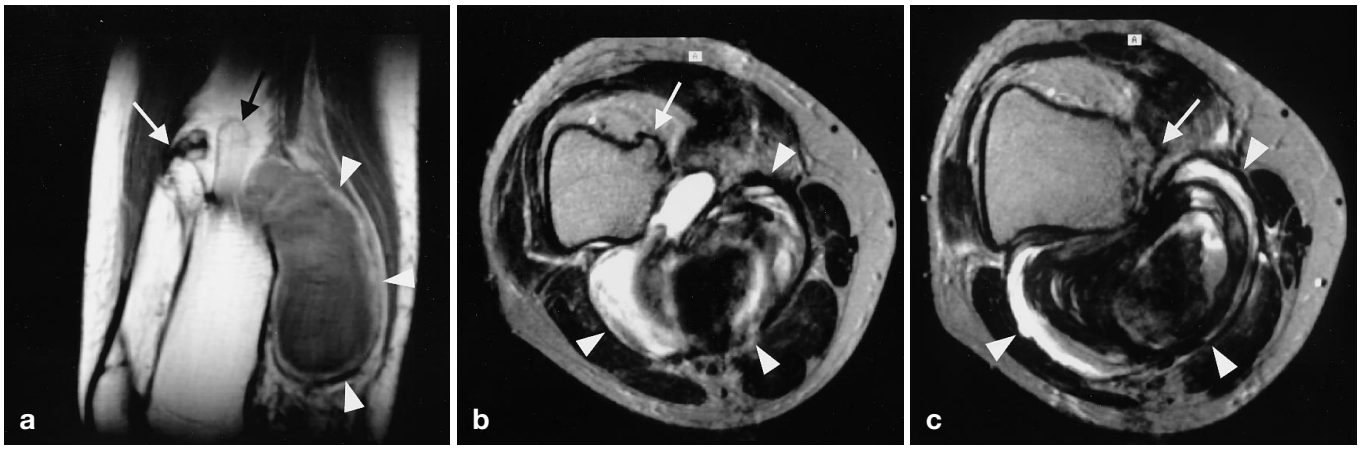

Fig. 8 a–c. A 22-year-old male patient with hereditary multiple exostoses who developed pain and a pulsatile mass in the distal femoral region. **a** Sagittal T1-weighted and **b,c** axial T2-weighted SE images demonstrate two pedunculated, completely ossified osteochondromas of the distal femur *(arrows)* as well as a large pseudoaneurysm *(arrowheads)* of the femoral artery. Note onion-skin-like appearance of thrombosed material within aneurysm on T2-weighted image **(c)**

the most commonly affected structure. Motor weakness or peroneal nerve palsy can occur as sequelae of chronic neural compression by osteochondromas located at the proximal tibiofibular articulation [6]. Palsies of the axillary and radial nerves have been described in patients with osteocartilaginous exostoses of the proximal humerus [21]. Magnetic resonance imaging is valuable to verify peripheral compressive neuropathies caused by osteocartilaginous exostoses. Changes in signal intensity, size, or position of the involved peripheral nerve have been shown to represent suggestive MR findings of compressive and entrapment neuropathies [22]. In advanced cases with muscle denervation MR images often show increased signal intensity of the corresponding muscle groups, progressing to muscular atrophy with fatty infiltration (Fig. 9) [22].

Spinal osteochondromas are uncommon, accounting for only 1–4 % of solitary osteochondromas and occurring in only 7–9 % of patients with hereditary multiple exostoses [2, 13, 23, 24, 25]. Osteochondromas of the spine predominate in the posterior elements but can occasionally originate from the vertebral body (Fig. 10) [2]. Possible symptoms due to compression of the spinal cord or nerve roots include myelopathy, paraplegia, radiculopathy, paraesthesia, and paresis [6, 13, 23, 24, 25, 26]. Anterior osteochondromas of the cervical spine can present with hoarseness and dysphagia [13, 23]. The neurocranium represents a very rare site of osteocartilaginous exostoses. Osteochondromas, which develop from the skull base or parasellar region, can occasionally become symptomatic with ataxic gait, visual disturbances, cranial nerve deficits, and headaches [6]. Magnetic resonance imaging represents the most informative imaging modality in patients with spinal or cranial osteochondromas. On the one hand, MR imaging can demonstrate typical morphologic features of this osteocartilaginous lesion, and therefore allows a definite differential diagnosis against other spinal or cranial masses; on the other hand, it offers detailed information on associated myelopathy (Fig. 10) and compression of nerve roots or intracranial structures [26]. As surgical planning requires an exact definition of the site of origin of spinal osteochondromas, section orientation should be modified dependent on the individual anatomic location in order to depict the location of continuity of the

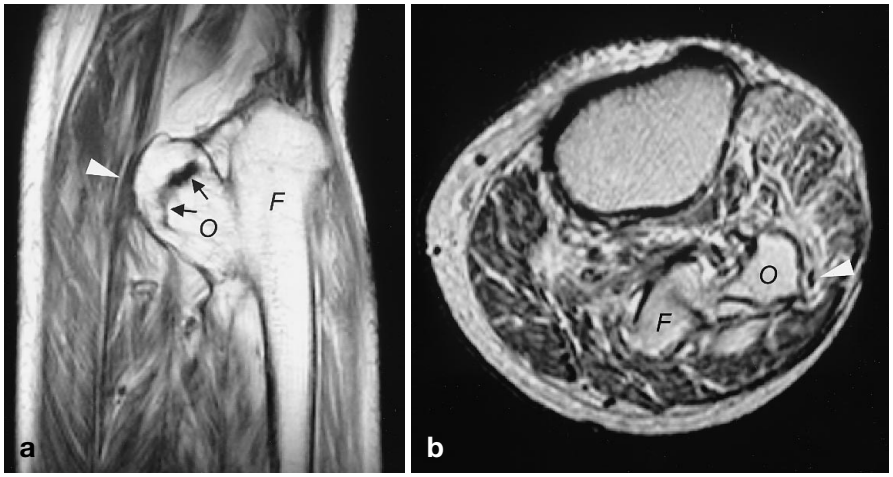

Fig. 9 a, b. A 58-year-old patient with peroneal nerve palsy. **a** Sagittal T1-weighted and **b** axial T2-weighted SE images show an osteochondroma *(O)* of the proximal fibula *(F)*. The former cartilage cap is completely ossified but is still distinguishable from the stalk by a line of low signal intensity *(arrows)*. Images depict contact to the common peroneal nerve *(arrowhead)*, which is displaced and slightly thickened. Note pronounced fatty atrophy of anterior extensor muscles

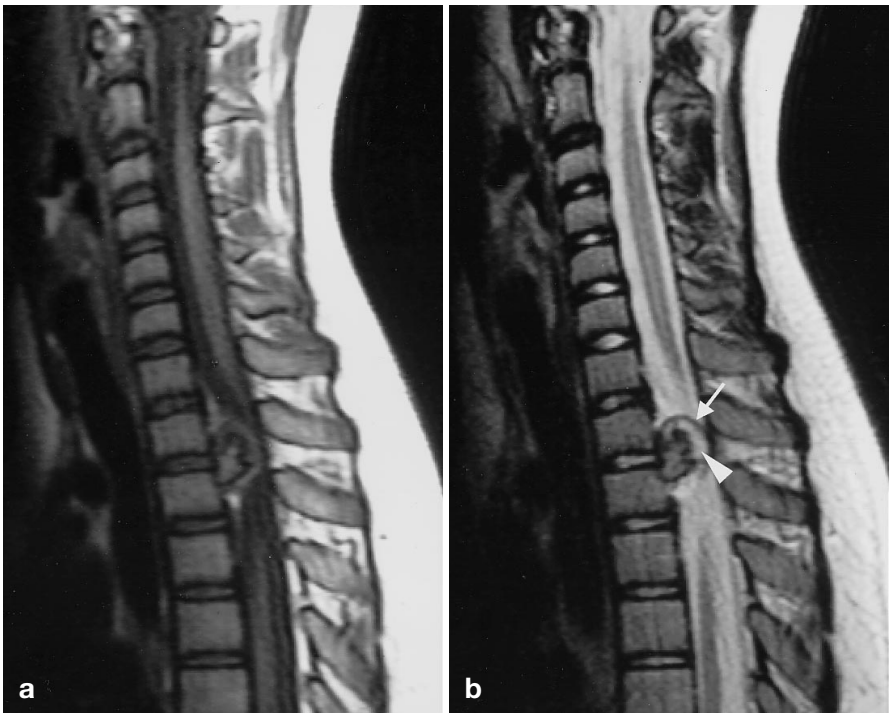

Fig. 10 a, b. A 14-year-old male patient with symptoms of progressive paraparesis. Sagittal **a** T1-weighted and **b** T2-weighted FSE images show an osteochondroma arising from the body of the second thoracic vertebra and causing compression of the spinal cord. Osseous and cartilaginous tumor components are clearly depicted. Note hyperintense signal of cartilage cap *(arrowhead)* on T2-weighted image **(b)** as well as hypointense lining *(arrow)*, indicating an intact perichondrium

osseous component with the vertebra (vertebral body, pedicle, posterior elements).

Malignant transformation

Malignant transformation represents the most worrisome complication, observed in approximately 1 % of patients with solitary osteochondromas and 5–25 % of patients with hereditary multiple exostoses. Sessile osteochondromas are more likely to undergo malignant transformation than pedunculated lesions [3]. The resulting malignant tumor most commonly is a chondrosarcoma ("secondary" or "exostotic" chondrosarcoma; Figs. 11, 12) [3, 6]. Painfulness or growth of an osteochondroma after skeletal maturity should always alert to the possibility of malignant transformation [2]. Cartilage cap thickness is an important criterion for differential diagnosis, since exostotic chondrosarcomas, which most often represent low-grade tumors, are difficult to diagnose as malignant on the basis of histologic findings alone [3, 5]. Malignancy should be suspected, if the thickness of the cap exceeds 2 cm in adults and 3 cm in children [5, 27]. Computed tomography and US have been applied in measuring cartilage cap thickness [5, 27, 28, 29, 30]. Computed tomography has been proven to be inaccurate, because it tends to underestimate the extent of the cartilage cap, which due to similar attenuation values is often indistinguishable from adjacent soft tissues [27, 29]. Ultrasound appears to be more reliable

Fig. 11 a–c. Exostotic chondrosarcoma of the right scapula in a 31-year-old female patient who presented with paravertebral pain and a palpable mass. Axial **a** T1-weighted, **b** T2-weighted, and **c** contrast-enhanced T1-weighted SE images show a cartilage cap with a thickness of more than 3 cm. Note hypointense septae *(arrows)* on T2-weighted image **(b)** as well as "ring-and-arc" and "septal" enhancement *(arrowheads)* on post-contrast T1-weighted image **(c)**. Histology confirmed a grade-1 chondrosarcoma arising in an osteochondroma

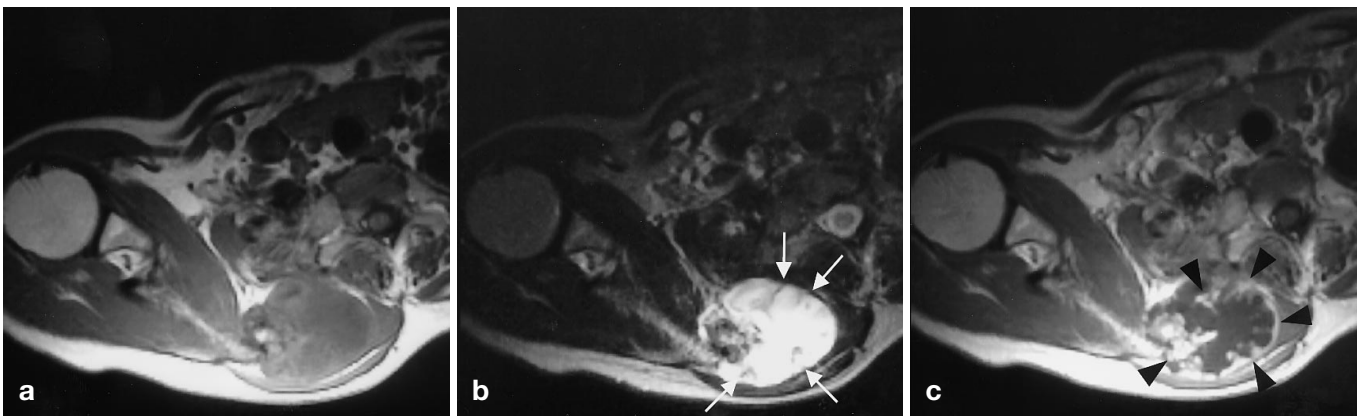

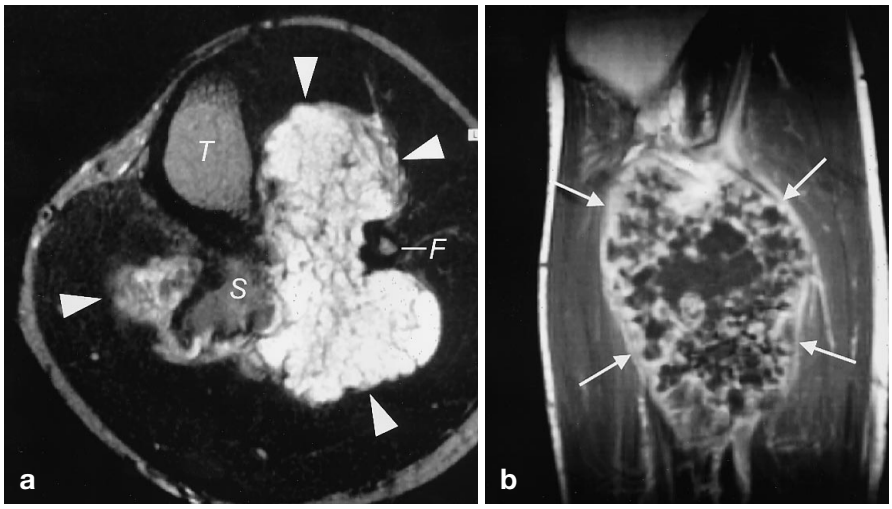

Fig. 12 a, b. Large secondary chondrosarcoma of the proximal tibia *(T)* in a 30-year-old male patient with pain and swelling of the right lower leg. **a** Axial T2-weighted SE image shows a lobulated, hyperintense mass *(arrowheads)* with hypointense septae. The tumor causes osseous destruction of the stalk *(S)* of the former osteochondroma and encases the fibula *(F)*. **b** On a sagittal contrast-enhanced T1-weighted SE image marked enhancement with "ring-and-arc" as well as "septal" pattern *(arrows)* is observed

in visualization and measurement of the cartilaginous cap, but shows substantial limitations in cases where the lesion is inwardly oriented, deeply located within soft tissues [30], or located in sites of complex skeletal anatomy (e. g., spine, thorax). Magnetic resonance imaging is the most accurate imaging modality for measurement of cartilage cap thickness, and therefore is the method of choice in cases which are suspect of malignant transformation [5, 29, 30], independent of the anatomic site of the lesion.

The presence of low signal intensity septa on T2-weighted images and "septal" or "ring-and-arc" enhancement on T1-weighted images after intravenous contrast administration (Figs. 11, 12) have been reported to represent additional criteria which suggest the diagnosis of a low-grade chondrosarcoma [8, 31, 32]. However, these features are discussed controversially in the literature, because they also are observed in benign cartilage-forming tumors [33].

Dynamic contrast-enhanced MR imaging studies using fast gradient-echo sequences have been applied with a view to differentiate benign from malignant bone lesions. In a preliminary investigation Geirnaerdt and coworkers reported fast dynamic MR imaging to be helpful in discrimination of benign (osteochondromas, enchondromas) and low-grade malignant cartilage tumors [34], although their study showed an overlap in early enhancement patterns of chondrosarcomas and osteochondromas in the immature skeleton. Van der Woude and coworkers, who among other bone tumors also studied cartilage-forming lesions, did not observe differences in enhancement onset, pattern, or progression, which could be used to accurately differentiate benign and malignant lesions [35]. Especially in the differential diagnosis of low-grade malignancies vs benign lesions they reported low sensitivities and specificities. Considering the facts that vascularity, on the one hand, is not a criterion for histopathological distinction between benign and malignant cartilaginous lesions [33], and gadolinium-enhanced MR images, on the other hand, depict tissue vascularization and perfusion rather than benignity or malignancy, we believe the use of static and dynamic contrast-enhanced sequences in the detection of malignant transformation of osteochondromas to remain questionable. Further studies on larger series of patients might prove helpful in evaluation of these imaging techniques.

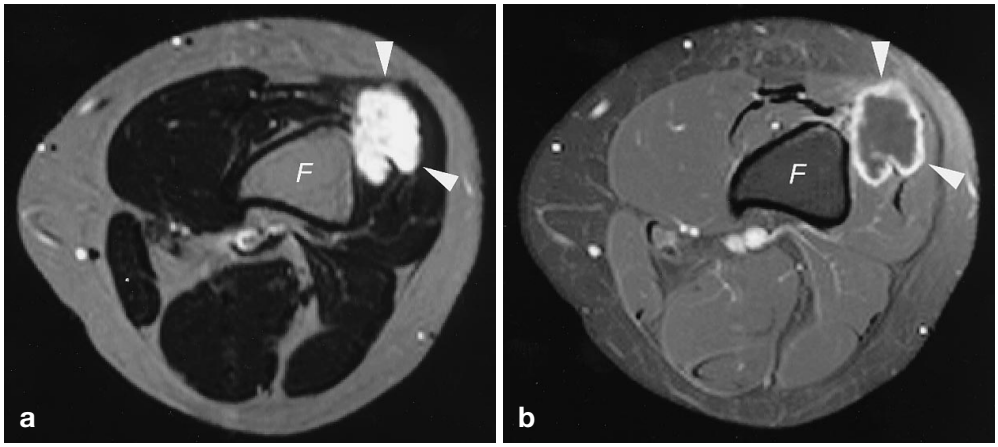

Fig. 13 a, b. A 21-year-old female patient with hereditary multiple exostoses who redeveloped pain and swelling after resection of an osteochondroma of the distal femur *(F)*. Magnetic resonance imaging depicts a lobulated mass *(arrowheads)* within the parosteal soft tissues, demonstrating hyperintense signal on axial **a** T2-weighted SE image and hypointense signal with marked peripheral enhancement on **b** fat-suppressed contrast-enhanced T1-weighted SE image. Surgery confirmed a recurrent cartilaginous tumor, which on histologic examination was diagnosed as a low-grade chondrosarcoma

Postoperative recurrence

Symptomatic osteochondromas usually require surgical removal. Resection has to include the entire cartilage cap with an intact periosteum, as postoperative recurrence of tumor growth may arise from hyaline cartilage or perichondrium left behind [5, 36]. Recurrence has been reported to occur in approximately 2% of cases following operative therapy [36]. Histologically, recurrent tumors can represent both, benign cartilaginous lesions and low-grade chondrosarcomas. Magnetic resonance imaging can be helpful in diagnosis of postoperative recurrence by detection of a parosteal mass with typical morphologic features of a cartilage-forming tumor (Fig. 13) and by ruling out other reasons for postoperative swelling or recurrent pain, such as seroma, abscess, and osteomyelitis.

References

1. Dahlin DC, Unni KK (1986) Osteochondroma (osteocartilaginous exostosis). In: Bone tumors, 4th edn: general aspects and data on 8452 cases. Thomas, Springfield, p. 18
2. Resnick D, Kyriakos M, Greenway GD (1989) Tumors and tumor-like lesions of bone: imaging and pathology of specific lesions. In: Bone and joint imaging. Saunders, Philadelphia, pp 1107–1181
3. Giudici MA, Moser RP, Kransdorf MJ (1993) Cartilaginous bone tumors. In: Imaging of bone and soft tissue tumors. Radiol Clin North Am 31: 237–259
4. Griffiths HJ, Thompson RC, Galloway HR, Everson LI, Suh JS (1991) Bursitis in association with solitary osteochondromas presenting as mass lesions. Skeletal Radiol 20: 513–516
5. Lee JK, Yao L, Wirth CR (1987) MR imaging of solitary osteochondromas: report of eight cases. AJR 149: 557–560
6. Karasick D, Schweitzer ME, Eschelman DJ (1997) Symptomatic osteochondromas: imaging features. AJR 168: 1507–1512
7. Cohen EK, Kressel HY, Frank TS et al. (1988) Hyaline cartilage-origin bone and soft-tissue neoplasms: MR appearance and histologic correlation. Radiology 167: 477–481
8. Geirnaerdt MJA, Bloem JL, Eulderink F, Hogendoorn PCW, Taminiau AHM (1993) Cartilaginous tumors: correlation of gadolinium-enhanced MR imaging and histopathologic findings. Radiology 186: 813–817
9. Uri DS, Dalinka MK, Kneeland JB (1996) Muscle impingement: MR imaging of a painful complication of osteochondromas. Skeletal Radiol 25: 689–692
10. Davids JR, Glancy GL, Eilert RE (1991) Fracture through the stalk of pedunculated osteochondromas: a report of three cases. Clin Orthop 271: 258–264
11. Harrison NK, Wilkinson J, O'Donohue J et al. (1994) Osteochondroma of the rib: an unusual cause of haemothorax. Thorax 49: 618–619
12. Russel EJ, Levy JM, Breit R, McMahan JT (1990) Osteocartilaginous tumors in the parapharyngeal space arising from bone exostoses. Am J Neuroradiol 11: 993–997
13. Arasil E, Erdem A, Yüceer N (1996) Osteochondroma of the upper cervical spine: a case report. Spine 21: 516–518
14. Shore RM, Poznanski AK, Anandappa EC, Dias LS (1994) Arterial and venous compromise by an osteochondroma. Pediatr Radiol 24: 39–40
15. Woolson ST, Maloney WJ, James DR (1989) Superficial femoral pseudoaneurysm and arterial thromboembolism caused by an osteochondroma. J Pediatr Orthop 9: 335–337
16. Lieberman J, Mazzucco J, Kwasnik E, Loyer R, Knight D (1994) Popliteal pseudoaneurysm as a complication of an adjacent osteochondroma. Ann Vasc Surg 8: 198–203
17. Longo JM, Rodriguez-Cabello J, Bilbao JI et al. (1990) Popliteal vein thrombosis and popliteal artery compression complicating fibular osteochondroma: ultrasound diagnosis. J Clin Ultrasound 18: 507–509
18. Harrington I, Campbell V, Valazques R, Williams T (1991) Pseudoaneurysm of the popliteal artery as a complication of an osteochondroma: a review of the literature and a case report. Clin Orthop Relat Res 270: 283–287
19. Ludwig WD, Yuh WTC, Montgomery WJ (1987) MR imaging of post-traumatic pseudoaneurysm of the deep femoral artery. J Comput Assist Tomogr 11: 1093–1095
20. Katayama Y, Tsubokawa T, Miyazaki S, Furuichi M, Hirayama T, Himi K (1991) Growth of totally thrombosed giant aneurysm within the posterior cranial fossa. Neuroradiology 33: 168–170
21. Witthaut J, Steffens KJ, Koob E (1994) Intermittent axillary nerve palsy caused by a humeral exostosis. J Hand Surg [Br] 19: 422–423
22. Beltran J, Rosenberg ZS (1994) Diagnosis of compressive and entrapment neuropathies of the upper extremity: value of MR imaging. AJR 163: 525–531
23. Albrecht S, Crutchfield JS, SeGall GK (1992) On spinal osteochondromas. J Neurosurg 77: 247–252
24. Gaetani P, Tancioni F, Merlo P, Villani L, Spanu G, Rodriguez y Baena R (1996) Spinal chondroma of the lumbar tract: case report. Surg Neurol 46: 534–539
25. Quirini GE, Meyer JR, Herman M, Russell EJ (1996) Osteochondroma of the thoracic spine: an unusual cause of spinal cord compression. Am J Neuroradiol 17: 961–964
26. Moriwaka F, Hozen H, Nakane K, Sasaki H, Tashiro K, Abe H (1990) Myelopathy due to osteochondroma: MR and CT studies. J Comput Assist Tomogr 14: 128–130
27. Hudson TM, Springfield DS, Spanier SS, Enneking WF, Hamlin DJ (1984) Benign exostoses and exostotic chondrosarcomas: evaluation of cartilage thickness by CT. Radiology 152: 595–599
28. Kenney PJ, Gilula LA, Murphy WA (1981) The use of computed tomography to distinguish osteochondroma and chondrosarcoma. Radiology 139: 129–137
29. Reuther G, Mutschler W (1989) Value of MRI versus CT and plain radiography in cartilage-forming tumors. Fortschr Röntgenstr 151: 647–652
30. Malghem J, Vande Berg B, Noel H, Maldague B (1992) Benign osteochondromas and exostotic chondrosarcomas: evaluation of cartilage cap thickness by ultrasound. Skeletal Radiol 21: 33–37
31. De Beuckeleer LHL, De Schepper AMA, Ramon F (1996) Magnetic resonance imaging of cartilaginous tumors: Is it useful or necessary? Skeletal Radiol 25: 137–141
32. De Beuckeleer LHL, De Schepper AMA, Ramon F, Somville J (1995) Magnetic resonance imaging of cartilaginous tumors: a retrospective study of 79 patients. Eur J Radiol 21: 34–40
33. Murphey MD, Flemming DJ, Boyea SR, Bojescul JA, Sweet DE, Temple HT (1998) Enchondroma versus chondrosarcoma in the appendicular skeleton: differentiating features. Radiographics 18: 1213–1237
34. Geirnaerdt MJ, Bloem JL, Van der Woude H, Taminiau AH, Hogendoorn PC (1996) Fast dynamic contrast-enhanced subtraction MR imaging allows differentiation of benign and low-grade malignant cartilaginous tumors. Radiology 201: 359
35. Van der Woude HJ, Verstraete KL, Hogendoorn PCW, Taminiau AHM, Hermans J, Bloem JL (1998) Musculoskeletal tumors: Does fast dynamic contrast-enhanced MR imaging contribute to the characterization? Radiology 208: 821–828
36. Forest M (1997) Osteochondroma. In: Forest M, Tomeno B, Vanel D (eds) Orthopedic surgical pathology: diagnosis of tumors and pseudotumoral lesions of bone and joints. Churchill Livingstone, Edinburgh, pp 177–189